Lateral Torsional and Longitudinal Buckling Analysis of Perforated Composite Plates

Ersin Demir[*]
[*]*Department of Mechatronis Engineering, Faculty of Technology, Pamukkale University, Denizli, Turkiye*
Corresponding author: +90 (258) 296 41 46, edemir@pau.edu.tr

Abstract

In this study, lateral and longitudinal buckling behaviors of perforated composite plates are investigated numerically. The composite plates are assumed to consist of two types of fabric, unidirectional and woven fabrics. The effects of changing the location, diameter and number of holes in the plate for unidirectional and woven fabric types on the lateral and longitudinal buckling strength are compared between the unperforated plate and each other. In addition, the effects of changing the fiber orientation angle on the lateral and longitudinal buckling load of the unidirectional fabric are also examined. Finally, the changes in the mode shape in two planes in lateral buckling and in a single plane in longitudinal buckling are shown, and the normalized amplitude change in the upper point of the free end of the plate is analyzed for different hole cases. In this study, the SolidWorks program is used for model design and the Simulation module of the SolidWorks program is used for numerical analysis.

Keywords: Buckling; Lateral; Plate; Perforated; Composite

1. Introduction

Composite structures are widely used in many areas of industry today. Since the basic materials considered can vary widely, studies on this subject are increasing day by day. In addition, different manufacturing defects such as separation or cracking etc. that occur in the manufacturing of composite structural elements are also the subject of researchers' study. These irregularities in the structure sometimes occur unintentionally and sometimes are done intentionally. For example, a composite plate may be drilled to pass the connections or to reduce the amount of material. However, this causes the strength of the plate under consideration to

change. Below, a literature research has been conducted on the lateral or longitudinal buckling behavior of plates or beams made of composite materials.

Hodges and Peters [1] considered composite strip-beam and I-beam. They developed a formula to obtain the lateral rotational buckling loads of their structures. They considered some parameters to be small to derive the formula. They also found that the formula gives accurate results as long as the parameters considered are small. Lee et al. [2] studied on the transverse buckling of I-section laminated composite beam. In their study, they developed a model based on the classical lamination theory. They obtained the critical buckling strength of the beam under central point, uniformly distributed and pure bending loads. Sapkas and Kollar [3] overcame the problem of lateral-torsional buckling of cantilever and simply supported composite beams. They examined three types of load cases in their calculations. These are concentrated end moments, concentrated forces and uniformly distributed load. They derived an explicit expression to solve the problem they were addressing. Hindman et al. [4] studied on the lateral torsional buckling behavior of plates made of wood material. They used four types of materials in their experimental studies. These materials are machine-stress-rated lumber, laminated veneer lumber, parallel strand lumber, and laminated strand lumber. They modified the load resistance factor design equation taken from the literature for laminated veneer lumber and laminated strand lumber materials to find better results. Lim and Shin [5] are derived the equations of motion and force-displacement relationships from the energy principle. Thumrongvut and Seangatith [6] experimentally investigated the lateral torsional buckling analyzes of pultruded fiber reinforced plastic cantilever channel beams. They compared the critical buckling moments obtained from the experiment with the results obtained from the modified steel design equation obtained from the standards. It has been understood that the equation gives appropriate values for slender beams, but not for short beams. Challamel and Girhammar [7] studied the lateral torsional behavior of laminated composite beams with

interlaminar shear. In their work, they presented closed-form solutions for composite beams under uniform bending moment. Horizontal and vertical shifts, which could not be included by simplifying the kinematic relations, were included with advanced kinematic assumptions to obtain more accurate lateral torsional buckling moment results. Additionally, in the study, a single lateral torsional buckling formula was derived depending on the horizontal and vertical connection parameters. Kim and Lee [8] dealt with the lateral buckling of the shear deformable laminated composite beams. They derived the geometrically non-linear theory for the lateral buckling of the composite beams. In order to demonstrate the validity of the study, they solved the lateral buckling of the beams numerically with the ABAQUS program, and compared the results that obtained from the numerical results with the results obtained from other researchers. Erkliğ et al. [9] investigated the effects of different perforate shapes on the lateral buckling behavior of composite beams. They made the calculation both experimentally and numerically. As a result of their study, they stated that the perforate shape was effective on lateral buckling. Rachchh et al. [10] are done the buckling analysis of the prepared composites experimentally and numerically using ANSYS to determine its buckling strength. Komur and Sonmez [11] conducted a numerical analysis on the buckling behaviors of perforated square and rectangular composite plates. Thus, they examined the effects of the aspect ratio of the plate, the length and the location of the edge load and hole diameter on the buckling behavior. Shams and Soltani [12] studied the buckling behavior of laminated composite plates reinforced with carbon nanotubes resting on Winkler-Pasternak elastic foundations. They performed the analysis using the reproducing kernel particle method based on first-order shear deformation theory. They determined the accuracy and convergence of their method by comparing their results with the results in the existing literature. Jiao et al. [13] discussed the theoretical study on the effect of geometries of wood composite I-beams with sinusoidal corrugated web on the buckling behavior. They also conducted experimental and numerical studies to verify their theoretical

work. Ahmadi [14] completed a thesis on lateral torsional buckling of anisotropic laminated composite beams subjected to various loading and boundary conditions. He derived the closed form buckling expressions in terms of the lateral, torsional and connection stiffness coefficients of the composite. He also investigated the buckling behavior of the beam according to different geometric and material parameters. He verified his analytical formulas with finite element solutions using ABAQUS. Bozkurt et al. [15] incorporated nano-clay particles into the epoxy resin in S glass/epoxy composites and thus investigated the lateral and axial buckling behaviors of the resulting composite samples experimentally. They examined the effects of different weight contents of nano-clay particle additives and fiber orientation angle in their studies. Sari et al. [16] performed buckling and free vibration analyzes of single and double composite Timoshenko beams. The double beams in their study are assumed to be connected by a layer of elastic translational and rotational springs. The eigenvalue problem they address is solved numerically by applying the Chebyshev spectral collocation method. Rossi et al. [17] examined the elastic behavior of Lateral Distortional Buckling in their study, and then they investigated the Lateral Distortional Buckling strength of steel-concrete composite beams. They also performed experimental investigation and nonlinear numerical analyzes to obtain the results. Erkmen et al. [18] developed a shear-deformable finite element formulation for lateral torsional buckling analysis of open-section fiber reinforced composite beams. Özbek [19] conducted an experimental study to investigate the effect of silica nanoparticles on the buckling behavior of Kevlar/epoxy fiber reinforced composite laminates. He performed both axial and lateral buckling tests in his work. He also analyzed critical areas of each sample using scanning electron microscope images following this test. Gao et al. [20] experimentally investigated the problem of lateral torsional buckling of steel-timber composite beam. The composite beam used in the experiment is constructed by bolting timber to either side of H-shaped steel. They also performed finite element analysis to reveal the failure mechanism of samples with different

geometric and physical parameters. Dehghani [21] overcome the nonlinear buckling and post-buckling problems of composite plates with the circular/elliptical cut-out. They used the Particle Semi-Energy method to solve the problem. Shaheen and Mahmoud [22] determined the critical moments of composite steel beams with various corrugated web profiles by using ANSYS 16 software. They predicted the failure load of a composite beam with various web profiles. Ding et al. [23] introduces a novel approach utilizing compactly supported radial basis functions to depict continuous fiber paths. This method facilitates the convenient association of manufacturing constraints, such as minimal turning radius and gap/overlap, with the curl operation and divergence of the fiber angle vector field. Deniz et al. [24] produced eight-layer composite laminates. In their study, they investigated how woven type, laminate designation and groove angles affect buckling behavior. Dias et al. [25] overcame the lateral distortion buckling of steel-concrete composite beams. They conducted four real-scale fire tests in their study. They also showed in their study that high temperatures increase the likelihood of lateral distortion buckling. Kumar and Kumar [26] investigated the critical buckling of a laminated porous composite plate using improved third-order shear deformation theory. Maji A. and Mahato [27] examined the buckling analysis of nonlinear behavior of first-order shear deformation laminated composite plates. They compared the results obtained from analytical solutions with exact and three-dimensional solutions. Farahani et al. [28] investigated the effect of the stacking sequence on buckling load of laminated composite rectangular plates on a Pasternak foundation under uniaxial and biaxial in-plane static loads. As a result of their studies, they determined the optimum orientation angles in different conditions.

As a result of the literature research, it was determined that the studies on lateral buckling were much less than the studies on longitudinal buckling. With this reason, in this study, the effects of changing the fabric type of the perforated composite plate and changing the fiber orientation angle on the lateral buckling strength, as well as the effects of changing the position, size and

number of holes on the lateral buckling strength are examined. Additionally, normalized mode shapes for lateral and longitudinal buckling are also examined.

2. Geometry and Material of the Plates

In this study, lateral torsional and longitudinal buckling analyzes of a composite plate are performed. Lateral torsional and longitudinal buckling of the considered plate are shown in Fig. 1a and b, respectively.

L, *b* and *t* shown in the figure are the length, width and thickness of the plate, respectively. As shown in the figure, when the force is applied to the upper right corner of the plate in the –y direction, it causes lateral torsional buckling, and when it is applied to the right side of the plate in the –x direction, it causes longitudinal buckling. When lateral torsional buckling occurs, the plate rotates with respect to both the *y* and *x* axes. These rotation angles are shown as α and β, respectively. These angular position changes are caused by bending and torsion effects acting on the plate. When longitudinal buckling occurs, the plate rotates only relative to the *y* axis. This rotation angle is shown as α. In this case the plate is only under bending effect.

In order to understand the effects of the location, diameter and number of holes in the composite plate on the mentioned buckling behaviors, three types of plates are considered as shown in Figure 2. The lengths of these plates are assumed to be L = 200 mm, their widths are b = 20 mm, and their thicknesses are t = 2.2 mm. It is also assumed that the composite plate has 8 layers. Additionally, the plates are assumed to have clamped free boundary conditions, as shown in Figure 1.

In the *L* type plate shown in Figure 2a, the hole diameter is taken as a constant 8 mm, and the distance between the center of the hole and the clamped end of the plate is changed from 25 mm to 175 mm with 25 mm intervals. As seen in Figure 2b, the hole in the *D* type plate is located at the center of the plate. In order to examine the change in hole diameter, the hole

diameter is enlarged from 4 mm to 16 mm with 4 mm intervals. In *N* type plate, there are three holes as seen in the Figure 2c. The distances between the centers of the holes are 50 mm. The hole diameter is increased from 4 mm to 16 mm in 4 mm intervals, as in the *D* type plates. Thus, the effect of increasing the number of holes can be examined by comparing *N* and *D* type plates. The composite plates are assumed to consist of two types of fabric. These are unidirectional and woven E-glass fabrics. The mechanical properties of these plates are given below [29].

Table 1 The material properties of the composite fabrics [29].

Fabrics	E_1 **[MPa]**	E_2 **[MPa]**	G_{12} **[MPa]**	$G_{13}= G_{23}$ **[MPa]**	ρ **[g/mm3]**	ν_{12}	$\nu_{13} = \nu_{23}$
Unidirectional	20443	5184	1856	1113	0.001526	0.36	0.09
Woven	21651	21651	1646	988	0.001578	0.35	0.35

3. Numerical Modelling and Analysis

The SolidWorks program is used for numerical analysis of the longitudinal and lateral torsional buckling of the plate. SolidWorks program has the ability to easily perform various structural analyses in addition to its ability to perform 2D and 3D design such as wireframes, plates, shells, and three-dimensional solid structures. Modeling, material assignment, loading, boundary condition definition, etc. operations can be applied quite easily. In addition, different analysis of a structural model such as static, buckling and vibration can be made with the Simulation Module running within the program. Moreover, the results obtained are quite satisfactory when compared with the results obtained from the other programs and experimental results. Before running the Simulation module for analysis, a 2D drawing of the plate in accordance with its dimensions is completed in the SolidWorks program, as seen in Figure 3a. The inside of the

frame that forms the edge lines of the plate, whose 2D drawing is made in Figure 3b, is selected and the wireframe model is converted into a plate structure.

After the modeling process is completed in the SolidWorks program, the Simulation module within the program is run. Buckling is selected as the analysis type in the Simulation Module section. Composite is selected as the structure material. Calculations of composite structures are made according to thick shell formulations. The thick shell formulation uses the Mindlin/Reissner model, which takes into account shear behavior. The material properties given in Table 1 are entered into the program. In addition, the number of layers of the composite material, the thickness of each layer, and layer orientations are also entered into the program. In addition to this, as seen in Figure 4, boundary condition is applied as clamped to left end of the plate and a 1 N lateral (Figure 4a) or longitudinal (Figure 4b) load is applied to the free end. The lateral load is applied to the upper right point, and the longitudinal load is applied to the right side. By applying a force of 1 N, the load factor required for the buckling load can be found. Additionally, as seen in the figure, the meshing process, which is mandatory in finite element-based programs, is also performed. In the meshing process, parabolic triangle type elements with six nodes, three at the corners and three at the middle edge, were used. Each node in the elements has six degrees of freedom, three translations and three rotations. When the results of the medium mesh and the fine mesh are compared, the medium mesh type is selected because there is no significant change in the results and in order not to slow down the process speed. In the medium mesh type, 1280 element numbers and 2737 node numbers are obtained for the unperforated plate. After the operations are completed, the simulation is run.

The 1st mode shapes obtained after completing the analysis in the simulation program are given in Figure 5. As seen in Figure 5a, the plate rotated in both the y-axis and x-axis with lateral torsional buckling. When Figure 5b is examined, it is seen that the plate rotates only in the y-axis with longitudinal buckling.

4. Result and Discussion

In this study, longitudinal and lateral torsional buckling behaviors of perforated composite plates are examined. The effects of fabric type, location of the hole, hole diameter, number of holes and fiber orientation angles are examined in detail below. Additionally, the bending and twisting angles occurring in the plate after lateral and longitudinal buckling are also examined.

4.1. Validation

To prove the accuracy of the results obtained from the SolidWorks-Simulation program, the experimental results in Reference [9] are considered. For this purpose, the material and geometric properties of perforated and unperforated composite laminated plates with $[(45/-45)_4]_s$ ply angle, the experimental results of which are given in the reference, are used and solved in the SolidWorks-Simulation program. The length, width and thickness of the plate used in the reference are 150 mm, 20 mm and 1.6 mm, respectively. The diameter of the circular hole and the length of one side of the square hole are 10 mm, and they are in the middle of the plate. In addition, the problem discussed in Reference [9] is also solved with the ANSYS program in order to prove the accuracy of the method used by the SolidWorks program. The experimental results in Reference [9] with present results obtained from SolidWorks-Simulation and ANSYS programs are compared in Table 2. When Table 2 is examined, it is seen that the results obtained from the Simulation program are quite close to the experimental results. In addition, when the results obtained from SolidWorks-Simulation and Ansys programs are compared, it is seen that the difference between them is almost zero percent. As a result, it can be said that both methods use similar solution techniques in solving lateral buckling of composite plates.

Table 2 Comparison of experimental and numerical results

Hole Status	Experiment Results [9]	Present Result (SolidWorks)	ANSYS Results	Percentage Difference (SolidWorks-ANSYS)	Percentage Error (Experimental-SolidWorks)
Unperforated	24.40	22.453	22.450	0.013	7.9795
	23.60				4.8602
	25.80				12.9729
Circular perforated	20.80	21.08	21.103	0.109	1.3462
	20.05				5.1372
	20.70				1.8357
Square perforated	19.06	20.384	20.413	0.142	6.9465
	18.93				7.6809
	19.85				2.6902

4.2. Effect of Fabric Types

Two types of fabric are used in this study. These are unidirectional (*U*) and woven (*W*) type fabrics. The lateral torsional and longitudinal buckling loads of unperforated, unidirectional and woven type plates are compared in Figure 6. The orientation angle of the fibers in these plates is 0 degrees. That is, in the unidirectional fabric the fibers are in the longitudinal direction of the plate, while in the woven fabric half of the fibers are in the direction of the longitudinal direction of the plate and the other half are perpendicular to it.

Interestingly, as seen in Figure 6, the woven type fabric is more durable than the unidirectional fabric in terms of longitudinal buckling strength, but less durable in terms of lateral torsional buckling strength. From the results obtained, it is understood that if high lateral torsional buckling strength is desired, unidirectional type fabric should be chosen. On the other hand, if high longitudinal buckling strength is desired, woven type fabric should be chosen.

4.3. Effect of Hole Location

In Figure 2a, it is considered to investigate the effect of the presence of the hole and the change in the location of the hole on the buckling strength of the composite plate.

As shown in Figure 7, lateral and longitudinal buckling analyzes are performed for composite plates with both unidirectional and woven fabrics. As seen from the figure, the presence of a hole on the plate reduced both lateral and longitudinal buckling strengths. This decrease is greater in local areas where the hole is especially close to the clamped end of the plate. When longitudinal buckling is examined, having the hole at 25 mm minimizes the strength, while in lateral buckling this situation is around 75 mm. While the longitudinal critical buckling load increases rapidly after 25 mm, the increase in lateral critical buckling load after 75 mm is relatively slow. In both cases, the effect of the presence of the hole at 175 mm of the plate on the buckling strength is negligible compared to the case without holes.

In addition, confirming the variation in Figure 6, woven fabric is more resistant to longitudinal buckling and unidirectional fabric is more resistant to lateral buckling. In addition, it can be said that the plate is generally more resistant to longitudinal buckling.

4.4. Effect of Hole Diameter

The presence of a hole in the plate and the increase in the diameter of this hole affects the buckling strength. The D-type plate model in Figure 2b is used to investigate this issue. As a result of the numerical analysis, the effect of increasing the hole diameter on both the lateral and longitudinal buckling strength of the plate with both fabric types is shown in Figure 8.

As can be seen from the figure, in all cases, increasing the hole diameter reduces both buckling strengths. However, this decrease is especially greater when the hole diameter is larger than 8 mm. Considering the presence of a hole in the middle of the plate and the enlargement of this hole, the plate is more resistant to longitudinal buckling than lateral buckling.

4.5. Effect of Hole Number

In order to understand the effect of increasing the number of holes in the plate on the buckling strength, the N-type plate in Figure 2c is used. As can be seen from the figure, there are three holes in the plate. Figure 9 shows the change in lateral and longitudinal critical buckling load by increasing the diameters of these three holes. It is seen in Figure 9 that, unlike Figure 8, all buckling values rapidly decrease to almost the same point.

It can be said that the difference between buckling loads is less. Especially as the hole diameter increased to 16 mm, the longitudinal buckling strength of the unidirectional plate decreases to the lowest level. Figure 10 is also examined to better understand the effects of increasing the number of holes on the buckling load.

Figure 10 shows the critical buckling load variations of unperforated, single-hole and three-hole plates. It is clearly seen in the figure that both lateral and longitudinal buckling strengths of unidirectional and woven plates decrease with the increase in the number of holes. This decrease is close to linear in all cases.

4.6. Effect of Fiber Orientation Angles

The effect of changing fiber angles in the unidirectional composite plate on the lateral and longitudinal critical buckling loads is shown in Figure 11. When investigating the effect of orientation angle on buckling loads, the change in hole position is first taken into account. When the longitudinal buckling load values in Figure 11 are examined, it is seen that the critical buckling loads decrease rapidly as the fiber rotation angle changes from 0° to 50°. However, it can be seen from the same figure that these load values remain almost constant after 50°. In addition, the critical buckling load characteristic of the unperforated plate is almost the same as that of the plate with a hole at a distance of 175 mm. The buckling load characteristic of the plate with a hole at a distance of 25 mm remains the same but is slightly lower than the others.

Figure 11 also shows the lateral torsional buckling characteristics in terms of the location of the hole. It is seen that the lateral torsional buckling load characteristics of both unperforated, 25 mm perforated and 175 mm perforated plates are the same. It can be seen that there is a rapid decrease form the 0° orientation angle to 30°, then it rises slightly until 60°, and then it decreases slightly again until 90°. In this buckling characteristic, as especially in longitudinal buckling, the buckling load values of the perforated plate at a distance of 25 mm are less than the others. The buckling values of unperforated and 175 mm perforated plates are almost the same.

Unlike Figure 11, in Figure 12, the variation of the orientation angle with the critical buckling load is evaluated in terms of the increase in hole diameter.

When Figure 12 is examined, it is understood that the lateral and longitudinal critical buckling load characteristics are similar to those shown in Figure 11. However, here, the plates whose buckling loads are very close to each other are unperforated and perforated plates with a diameter of 4 mm. In addition, although the buckling load characteristic remains approximately the same in the plate with a hole diameter of 16 mm, the load values are lower than the others.

In the plates shown in Figure 13, the number of holes is increased to three and the hole diameters are increased. The only difference between the plates in Figure 13 and those in Figure 12 is that the number of holes is increased to three. When the two figures are compared, it is seen that the critical buckling load of the perforated plates with a diameter of 16 mm decreases even more. Similar to Figure 12, both lateral and longitudinal critical buckling load values of the unperforated and 4 mm perforated plates are quite close to each other.

4.7. Mode Shape

When the mode shapes obtained as a result of the buckling analysis of the plate are examined, it is understood that the location, diameter and number of holes affect the mode shape. Below,

these effects affecting the mode shape are evaluated for lateral and longitudinal buckling analysis.

4.7.1. Lateral Buckling

As seen in Figure 1a, when lateral buckling occurs, the beam rotates with respect to both *x* and *y* axes. Therefore, the mode shape is examined according to two axes. In order to see the mode shape according to the *x*-*z* plane, data is taken along the upper edge of the plate, and the top view of the plate after buckling for unidirectional and woven fabric types is given in Figure 14a. In Figure 14b, data are taken along the edge in the height direction at the free end of the plate, and the mode shape in the *y*-*z* plane is shown by giving the front view of the plate. The data given in both figures are normalized values.

When Figure 14a is examined, the first mode shapes in the *x*-*z* plane for unidirectional and woven fabric are quite close to each other. When the mode shape in the *y*-*z* plane is examined in Figure 14b, it is seen that the end edge of the plate remains linear and rotates relative to the *x* axis. In addition, it is seen that the mode shapes of unidirectional and woven type fabrics are similar to each other, but there is a difference in value.

Figure 15 shows the effect of hole location on the mode shape. For this purpose, the amplitude value of the upper point of the free end of the plate is taken as basis. The general mode shape is not given because the values are very close to each other, instead the upper point of the free end where the maximum amplitude occurs is taken into account. In order to see the general behavior of the variation in the hole location, the cases where the hole is close to the edge of the clamped boundary (25 mm), the hole is in the middle (100 mm), and the hole is close to the free end (175 mm) are examined. As seen in Figure 15, the amplitude increased as the hole is closer to the clamped edge, and as the hole approached the free end, the amplitude values decreased and even reached almost the amplitude of the non-perforated plate. It is also seen that the amplitude occurring in woven type fabric is lower than in unidirectional fabric. Accordingly,

it can be said that the buckling strength of woven fabric is higher and if high buckling strength is desired, the hole should not be brought closer to the clamped end.

The effect of increasing hole diameter on amplitude is shown in Figure 16. As can be seen from the figure, while the hole diameter increased from 4 mm to 12 mm, the amplitude value decreased slightly. When the hole diameter is 16 mm, the amplitude value increased slightly. When examined in general, it is understood that increasing the hole diameter does not cause much change in the amplitude value. It is also seen that the amplitude values in woven fabric are lower than in unidirectional fabric.

In Figure 17, there are three holes in the plate and the diameters of these holes have been increased. In this figure, it is seen that the amplitude values in the woven type fabric are less than in the unidirectional fabric, similar to the behavior in the previous figure. However, unlike the previous figure, the amplitude values increased parabolically as the hole diameters increased.

4.7.2. Longitudinal Buckling

The mode shape in longitudinal buckling is shown in Figure 1b. As can be seen from the figure, rotation occurs only relative to the *y* axis. That is, there is a change in amplitude only in the *x*-*z* plane. So, data is taken along the top edge of the plate. Figure 18 shows the top view of the plate after buckling for unidirectional and woven fabric types.

When Figure 18 is examined, the first mode shapes in the *x*-*z* plane for unidirectional and woven fabric are quite close to each other, as in Figure 14a.

Figure 19 shows the effect of the hole location on the normalized amplitude of the free end of the plate in case of longitudinal buckling. Normalized amplitude values were obtained from the upper point of the free end of the plate. As can be seen from Figure 19, the values are very close to each other. In addition, although the difference is small, it is seen that the amplitude value of

the plate increases when the hole is close to the clamped edge. This increase is also observed in Figure 15. However, unlike Figure 15, when the hole was at the midpoint, the amplitude value was obtained lower than that of the plate without hole. When the hole location approaches the free end, the value obtained is almost the same as the value obtained from the plate without a hole.

Figure 20 shows the effect of the variation in hole diameter on the normalized amplitude. It can be seen from the figure that the amplitude at the free end of the plate decreases as the hole diameter increases for both unidirectional and woven fabrics. The values obtained for unidirectional and woven fabrics are very close to each other.

When compared with Figure 16, it can be seen that increasing the hole diameter affects the amplitude in the case of longitudinal buckling, unlike lateral buckling. It can be seen from Figure 20 that the amplitude values decreased parabolically, especially when the hole diameter was larger than 8 mm.

The amplitude variation obtained when there are three holes in the plate and the diameters of the holes are increased is given in Figure 21. It can be seen that the curve trend obtained from the three-hole plate is similar to that obtained from the single-hole plate.

5. Conclusion

In this study, the lateral and longitudinal buckling behaviors of perforated composite plates are investigated and the following results are obtained.

- While the lateral buckling strength of the unidirectional composite plate is higher than the woven composite plate, but its longitudinal buckling strength is lower.
- The presence of a hole on the plate reduces both lateral and longitudinal buckling strength. When the hole location is very close to the clamped end, the longitudinal

buckling strength decreases to the minimum level. This value for lateral buckling strength is obtained approximately near the middle region of the plate.

- Increasing the hole diameter reduces both lateral and longitudinal buckling strength. However, this decrease is more effective after 8 mm.
- Increasing the number of holes reduces the lateral and longitudinal buckling strengths in a nearly linear rate. In addition, when the plates with a large number of holes are compared, it is seen that the fastest decrease is in the longitudinal buckling strength of the unidirectional composite plate.
- Longitudinal buckling strength decreases by changing the fiber orientation angle from 0° to 50°. But it remains almost constant between 50° and 90°. As for the lateral buckling strength, it decreases with changing the fiber orientation angle from 0° to 30°. However, it increases slightly when changing from 30° to 60°. It then decreases slightly again when changing from 60° to 90°.
- When the mode shapes are examined in the case of lateral torsional buckling, the amplitude values obtained from the unidirectional fabric plate are higher than those obtained from the woven fabric plate. In the case of longitudinal buckling, it is almost the same in these two fabric types.
- In the case of lateral buckling, when the hole position is close to the clamped edge of the plate, the amplitude value increases slightly, while as the hole position moves away, it is around the amplitude value of the unperforated sample. In the case of longitudinal buckling, unlike the case of lateral buckling, the amplitude value decreased slightly when the hole location is in the middle of the plate.
- While increasing the hole diameter did not affect the amplitude value much in the case of lateral buckling, it decreases the amplitude value in the case of longitudinal buckling.

- While increasing the multiple hole diameter increases the amplitude value in the case of lateral buckling, on the contrary, it decreases the amplitude value in the case of longitudinal buckling.

References

[1] Hodges D.H. and Peters D.A. "Lateral-torsional buckling of cantilevered elastically coupled composite strip- and I-beams", *Int. J. Solids Struct.,* **38**(9), pp. 1585-1603 (2001). DOI: https://doi.org/10.1016/S0020-7683(00)00111-6.

[2] Lee J., Kim S.E. and Hong K. "Lateral buckling of I-section composite beams", *Eng. Struct.,* **24**(7), pp. 955-964 (2002). DOI: https://doi.org/10.1016/S0141-0296(02)00016-0.

[3] Sapkas A. and Kollar L.P. "Lateral-torsional buckling of composite beams", *Int. J. Solids Struct.,* **39**(11), pp. 2939-2963 (2002). DOI: https://doi.org/10.1016/S0020-7683(02)00236-6.

[4] Hindman D.P., Manbeck H.B. and Lanowiak J.J. "Measurement and prediction of lateral torsional buckling loads of composite wood materials: Rectangular sections", *For. Prod. J.,* **55**(9), pp. 42-47 (2005).

[5] Lim N.I. and Shin D.K. "Dynamic stiffness matrix for flexural-torsional, lateral buckling and free vibration analyses of mono-symmetric thin-walled composite beams", *Int. J. Struct. Stab. Dyn.,* **9**(3), pp. 411-436 (2009). DOI: https://doi.org/10.1142/S0219455409003107.

[6] Thumrongvut J. and Seangatith S. "Experimental Study on Lateral-Torsional Buckling of PFRP Cantilevered Channel Beams", *Procedia Eng.*, **14**, pp. 2438-2445 (2011). DOI: https://doi.org/10.1016/j.proeng.2011.07.306.

[7] Challamel N. and Girhammar U.A. “Lateral-torsional buckling of vertically layered composite beams with interlayer slip under uniform moment”, *Eng. Struct.*, **34**, pp. 505-513 (2012). DOI: https://doi.org/10.1016/j.engstruct.2011.10.004.

[8] Kim N.I. and Lee J. “Lateral buckling of shear deformable laminated composite I-beams using the finite element method”, *Int. J. Mech. Sci.*, **68**, pp. 246-257 (2013). DOI: https://doi.org/10.1016/j.ijmecsci.2013.01.023.

[9] Erkliğ A., Yeter E. and Bulut M. “The effects of cut-outs on lateral buckling behavior of laminated composite beams”, *Compos. Struct.*, **104**, pp. 54-59 (2013). DOI: https://doi.org/10.1016/j.compstruct.2013.04.019.

[10] Rachchh N.V., Misra R.K. and Roychowdhary D.G. “Effect of red mud filler on mechanical and buckling characteristics of coir fibre-reinforced polymer composite”, *Iran. Polym. J.*, **24**, pp. 253-265 (2015). DOI: https://doi.org/10.1007/s13726-015-0317-4.

[11] Komur M.A. and Sonmez M. “Elastic buckling behavior of rectangular plates with holes subjected to partial edge loading”, *J. Constr. Steel Res.*, **112**, pp. 54-60 (2015). DOI: https://doi.org/10.1016/j.jcsr.2015.04.020.

[12] Shams S. and Soltani B. “Buckling of Laminated Carbon Nanotube-Reinforced Composite Plates on Elastic Foundations Using a Meshfree Method”, *Arab. J. Sci. Eng.*, **41**(5), pp. 1981-1993 (2016). DOI: https://doi.org/10.1007/s13369-016-2051-4.

[13] Jiao P., Borchani W., Soleimani S. and McGraw B. “Lateral-torsional buckling analysis of wood composite I-beams with sinusoidal corrugated web”, *Thin-Walled Struct.*, **119**, pp. 72-82 (2017). DOI: https://doi.org/10.1016/j.tws.2017.05.025.

[14] Ahmadi H. “Lateral torsional buckling of anisotropic laminated composite beams subjected to various loading and boundary conditions”, *PhD. Thesis, Kansas State University, Manhattan, Kansas*; (2017).

[15] Bozkurt Ö.Y., Bulut M., Erkliğ A. and Faydh W.A. "Axial and lateral buckling analysis of fiber reinforced S-glass/epoxy composites containing nano-clay particles", *Compos. B Eng.*, **158**, pp. 82-91 (2019). DOI: https://doi.org/10.1016/j.compositesb.2018.09.043.

[16] Sari M.S., Al-Kouz W.G. and Al-Waked R. "Bending–torsional-coupled vibrations and buckling characteristics of single and double composite Timoshenko beams", *Adv. Mech. Eng.*, **11**(3), pp. 1-16 (2019). DOI: https://doi.org/10.1177/1687814019834452.

[17] Rossi A., Nicoletti R.S., Clemente de Souza A.S. and Martins C.H. "Lateral distortional buckling in steel-concrete composite beams: A review", *Struct.*, **27**, pp. 1299-1312 (2020). DOI: https://doi.org/10.1016/j.istruc.2020.07.026.

[18] Erkmen R.E., Niki V. and Afnani A. "Shear-deformable hybrid finite-element formulation for lateral-torsional buckling analysis of composite thin-walled members", *Can. J. Civ. Eng.*, **48**(1), pp. 1026 -1036 (2021). DOI: https://doi.org/10.1139/cjce-2019-0560.

[19] Özbek Ö. "Axial and lateral buckling analysis of kevlar/epoxy fiber-reinforced composite laminates incorporating silica nanoparticles", *Polym. Compos.*, **42**, pp. 1109-1122 **(**2021). DOI: https://doi.org/10.1002/pc.25886.

[20] Gao Y., Xu F., Meng X., Zhang Y. and Yang H. "Experimental and numerical study on the lateral torsional buckling of full-scale steel-timber composite beams", *Adv. Struct. Eng.*, **25**(3), pp. 522-540 (2022). DOI: https://doi.org/10.1177/13694332211057263.

[21] Dehghani M. "A particle method development for analyzing the post-buckling behavior of composite plates with a cut-out", *Sci. Iran.*, **28**(4) , pp. 2176-2186 (2021). DOI: https://doi.org/10.24200/sci.2021.55993.4506.

[22] Shaheen Y.B.I. and Mahmoud A.M. “Lateral-torsional buckling resistance of composite steel beams with corrugated webs”, *Struct. Eng. Mech.*, **81**(6), pp. 751-767 (2022). DOI: https://doi.org/https://doi.org/10.12989/sem.2022.81.6.751.

[23] Ding H., Xu B., Song L., Li W. and Huang X. “Buckling optimization of variable-stiffness composites with multiple cutouts considering manufacturing constraints”, *Adv. Eng. Softw.*, **174**, , (2022). DOI: https://doi.org/10.1016/j.advengsoft.2022.103303.

[24] Deniz M.E., Bardakci R. and Aydin F. “Buckling in rectangular hybrid composite plates with angled groove-shaped cut-outs”, *Mater. Test.*, **65**(3), pp. 332-345 (2023). DOI: https://doi.org/10.1515/mt-2022-0317.

[25] Dias J.V.F., Siciliano B.M., Nery L.S., Caldas R.B. and Fakury R.H. “Lateral distortional buckling of continuous composite beams in fire situation: Experimental and numerical analyses”, *Fire Saf. J.*, **140**, (2023). DOI: https://doi.org/10.1016/j.firesaf.2023.103893.

[26] Kumar R. and Kumar A., “Uniaxial buckling of laminated composite porous plate”, *Multiscale Multidiscip. Model. Exp. Des.*, (2023). DOI: https://doi.org/10.1007/s41939-023-00284-4.

[27] Maji A. and Mahato P.K. “Buckling Analysis of Nonlinear First-Order Shear Deformation Composite Plates” *Machines, Mechanism and Robotics, Conference paper*, pp. 609–621 (2021). DOI: https://doi.org/10.1007/978-981-16-0550-5_60.

[28] Farahani S., Fathi M. and Nazarimofrad E. “Three effect of buckling and post-buckling behavior of laminated composite plates with rotationally restrained and Pasternak foundation on stacking sequence optimization” *Sci. Iran.*, **28**(4), pp. 2053-2069 (2021). DOI: https://doi.org/10.24200/sci.2020.55883.4453.

[29] Demir E. “A study on natural frequencies and damping ratios of composite beams with holes”, *Steel and Compos. Struct.*, **21**(6), pp. 1211-1226 (2016). DOI: https://doi.org/10.12989/scs.2016.21.6.1211.

Author Biography

E. Demir is an Associate Professor at the Mechatronics Engineering Department in the Technology Faculty of Pamukkale University, Türkiye. He completed his PhD degree in Mechanical Engineering from Pamukkale University, Türkiye in 2009. He is specialized in structural analyses (buckling or vibrations ect.) of structural elements (functionally graded materials, composite materials ect.) and has conducted different studies especially on composite materials and published them in different scientific journals. These studies include theoretical, experimental or numerical studies.

List of Figures

List of Tables

FIGURES

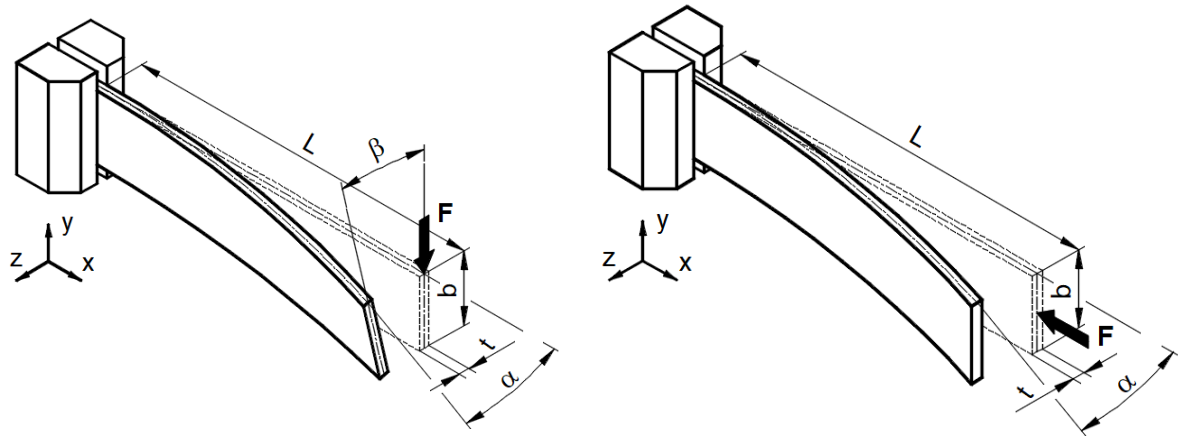

(a) Lateral torsional buckling (b) Longitudinal buckling

Fig. 1 Types of buckling occurring in the plate

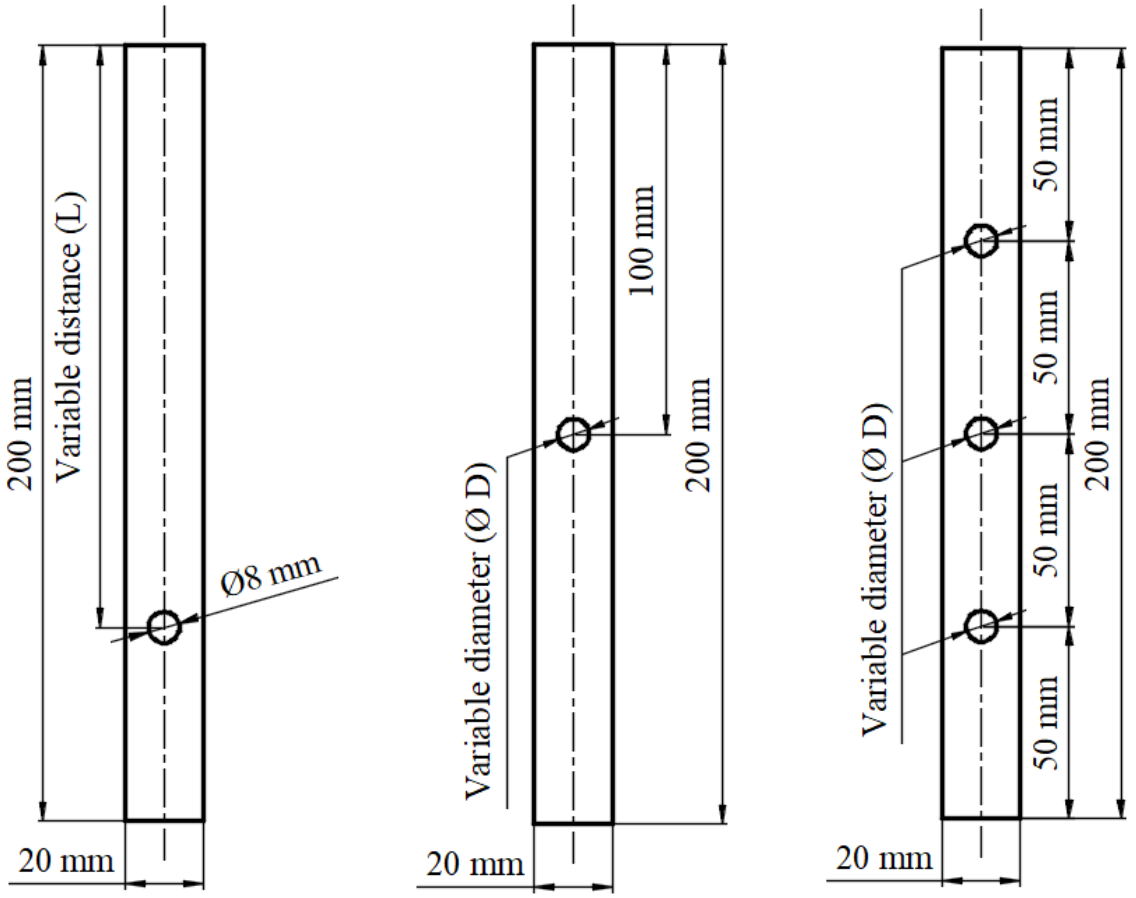

(a) *L* Type (b) *D* Type (c) *N* Type

Fig. 2 Plate Types

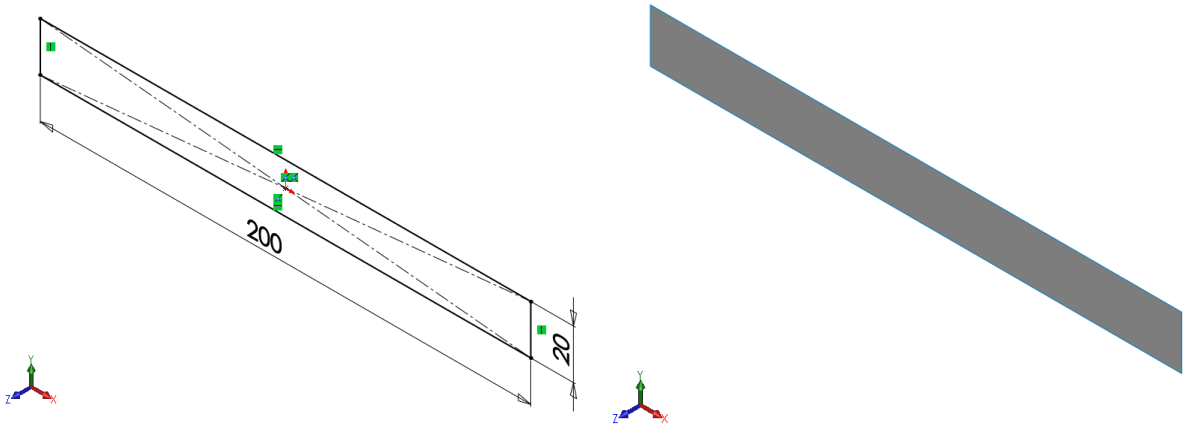

(a) 2D wireframe model (b) 2D plate structure

Fig. 3 Modeling with SolidWorks program

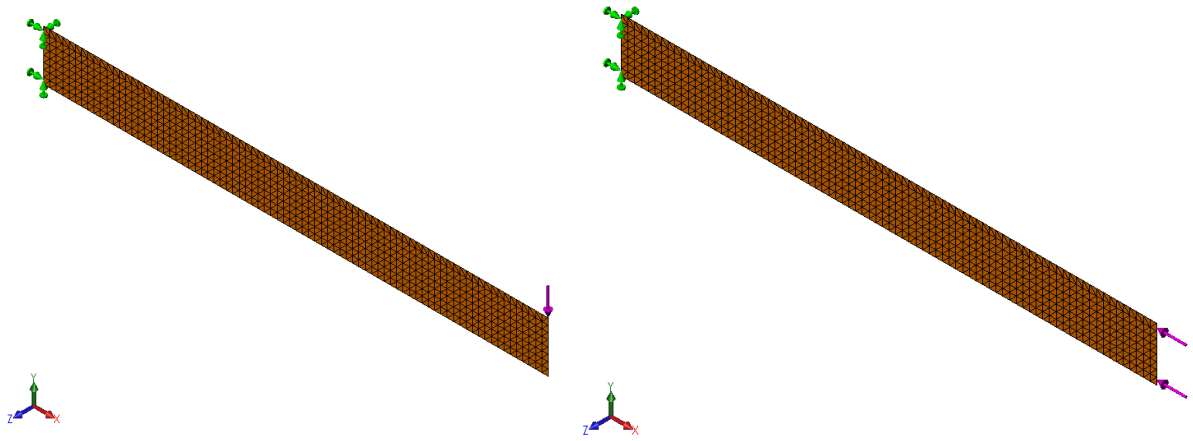

(a) under lateral loads (b) under longitudinal loads

Fig. 4 Meshed models

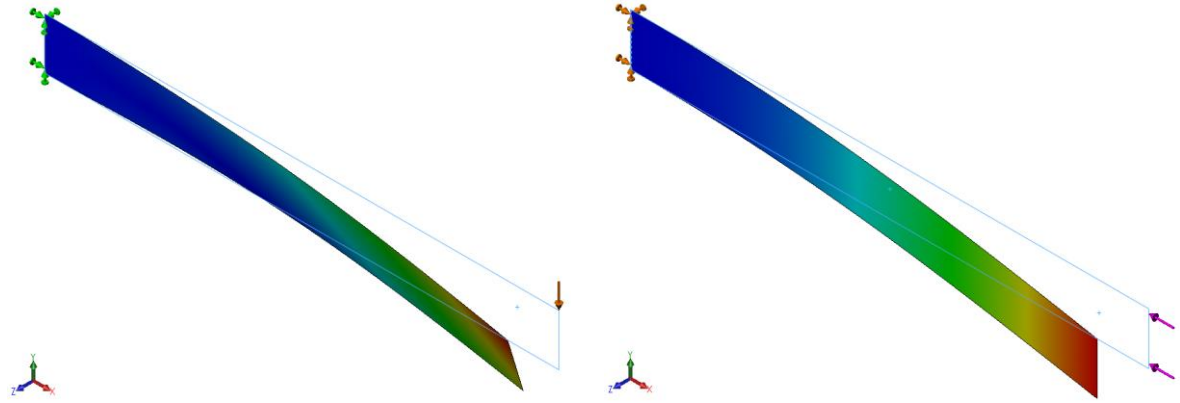

(a) lateral torsional buckling (b) longitudinal buckling

Fig. 5 1st mode shape of the buckling after analysis

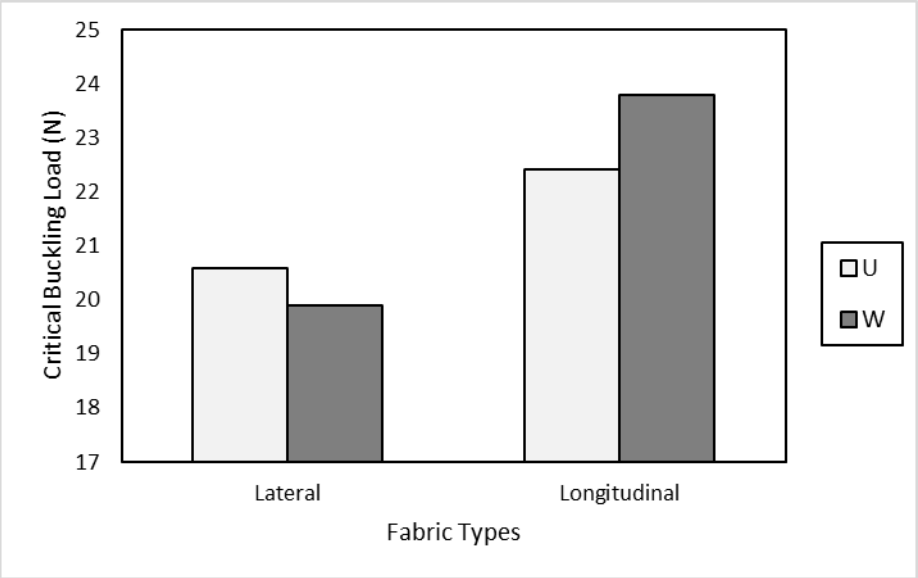

Fig. 6 Variations in lateral and longitudinal buckling loads of the plates with the different fabric types

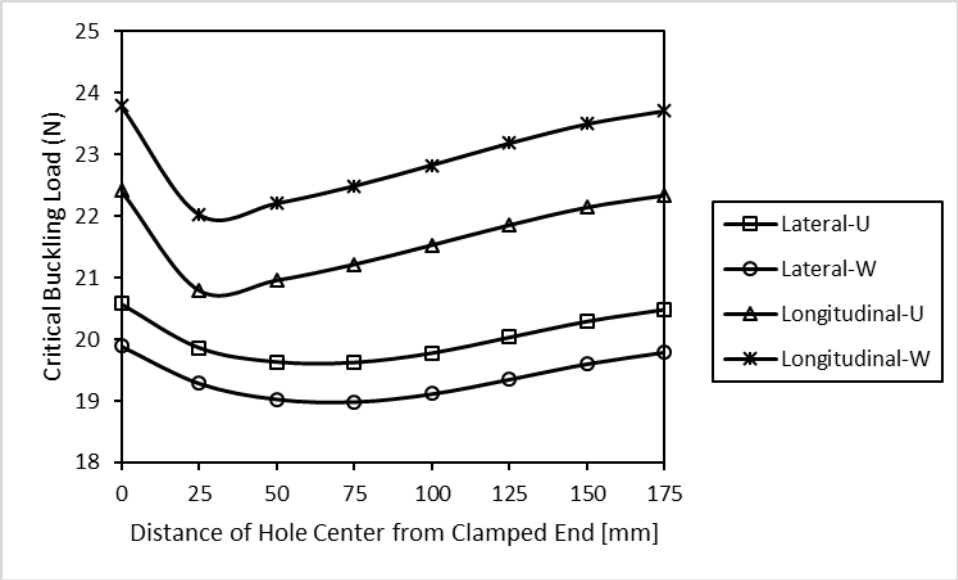

Fig. 7 Variations in buckling load of the plates by changing the hole location

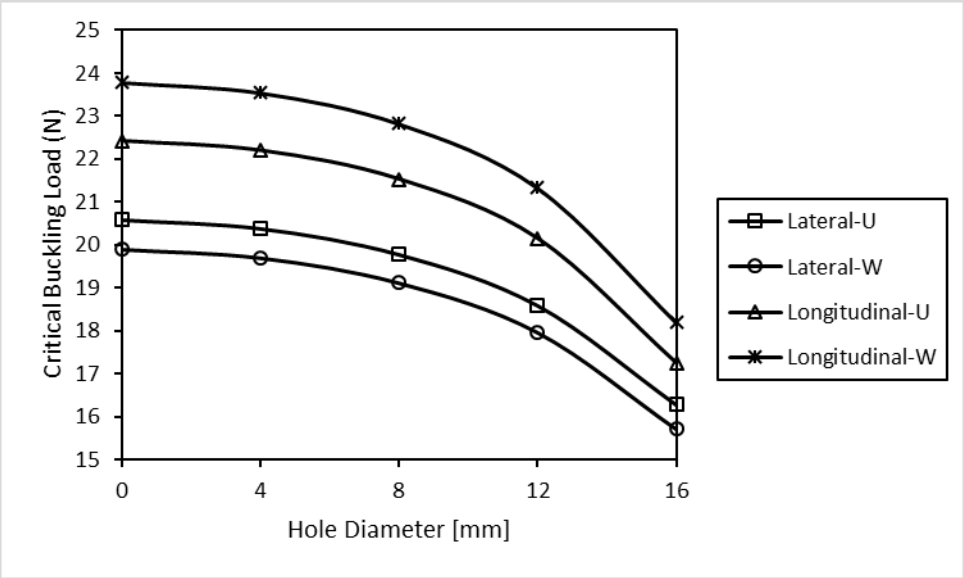

Fig. 8 Variations in buckling load of the plates with increasing the hole diameter

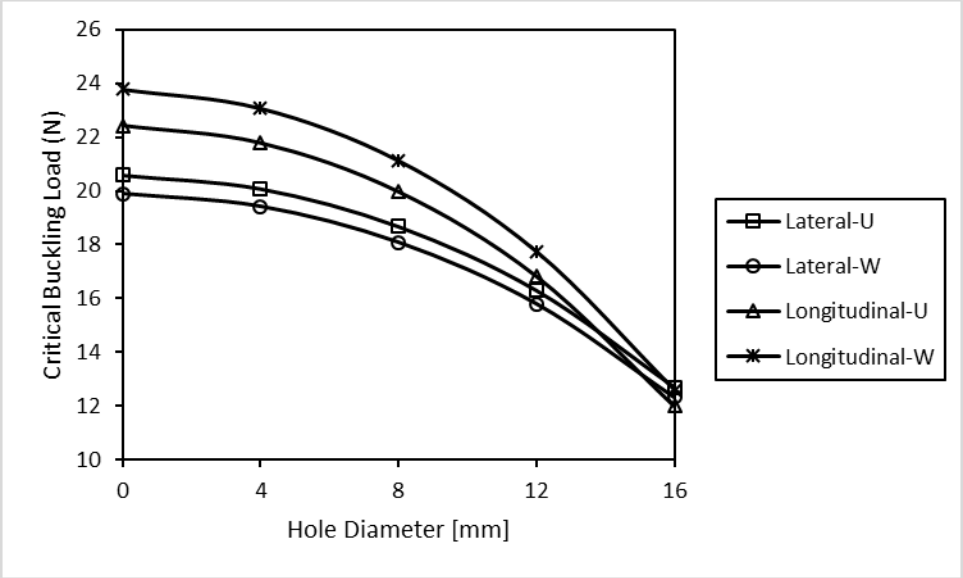

Fig. 9 Variations in buckling load of the plate with increasing diameters of three holes

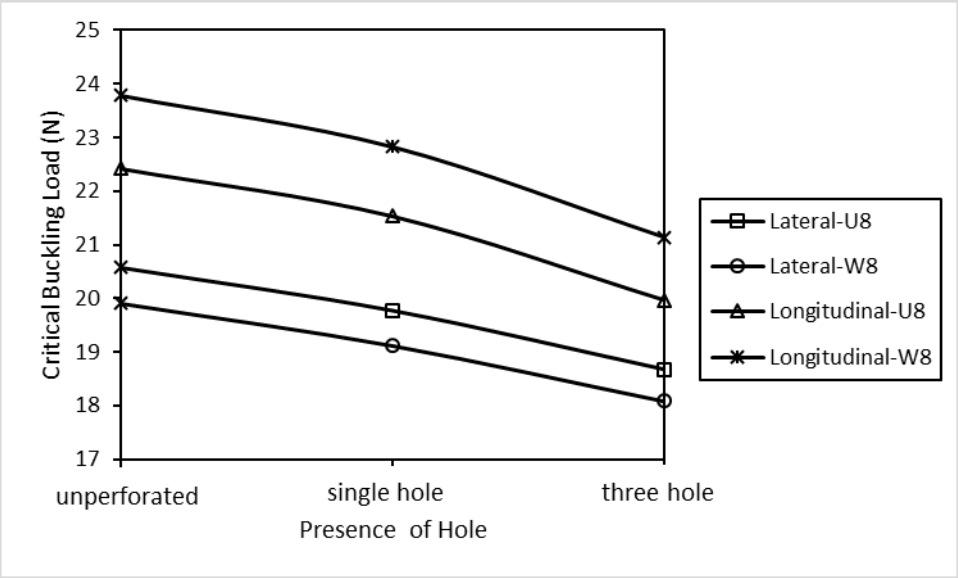

Fig. 10 Variations in buckling load of the plates with increasing number of holes

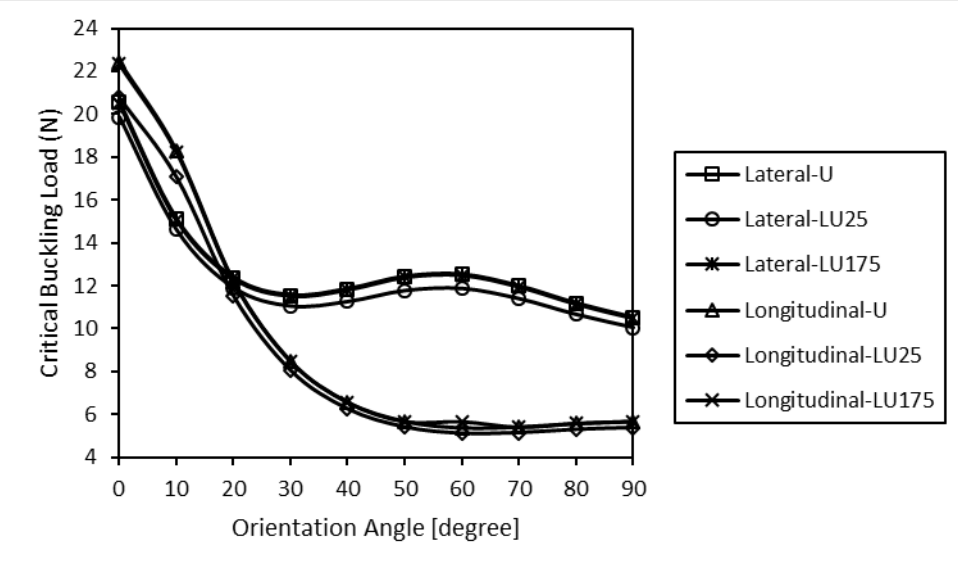

Fig. 11 Variations in buckling load of the plates versus orientation angle and hole location

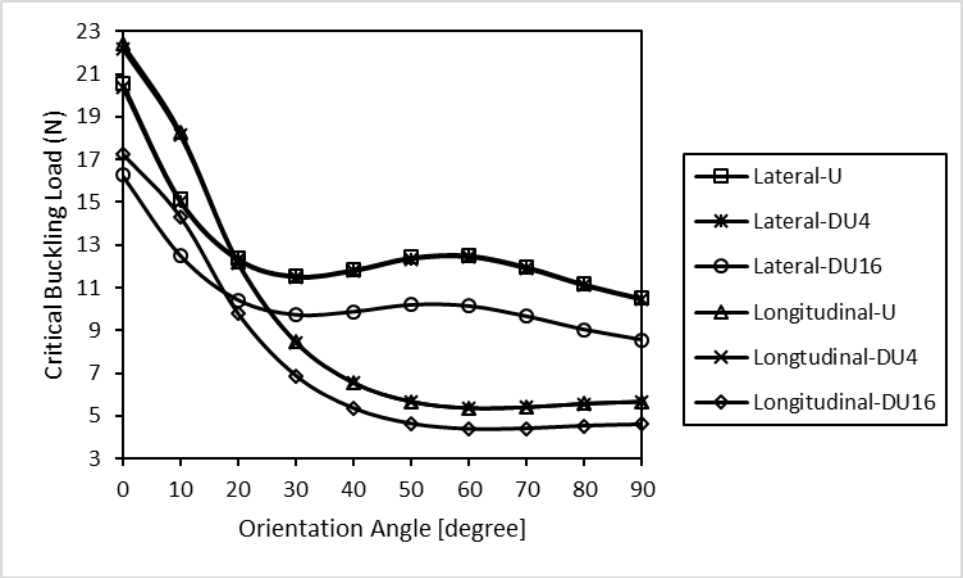

Fig. 12 Variations in buckling load of the plates versus orientation angle and hole diameter

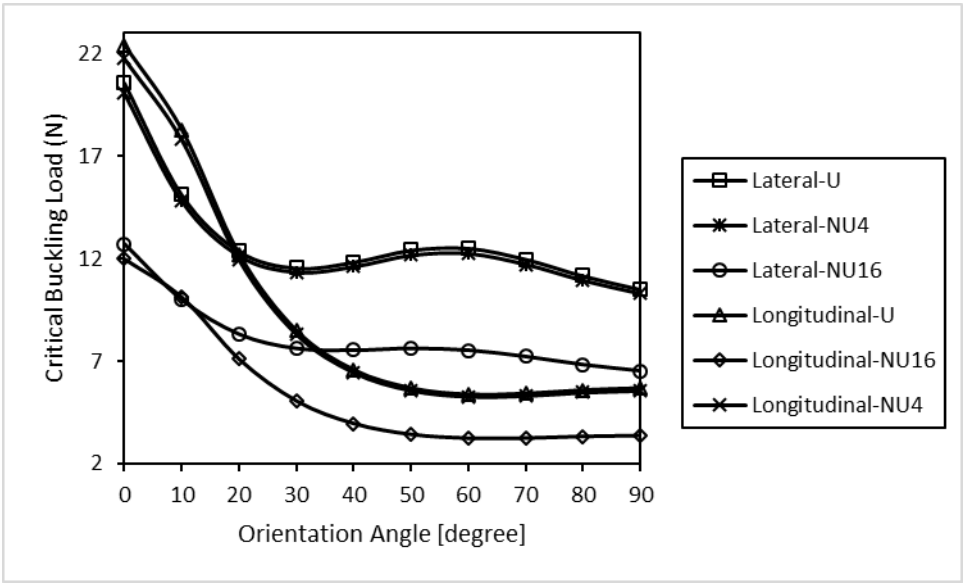

Fig. 13 Variations in buckling load of the plates versus orientation angle and hole number

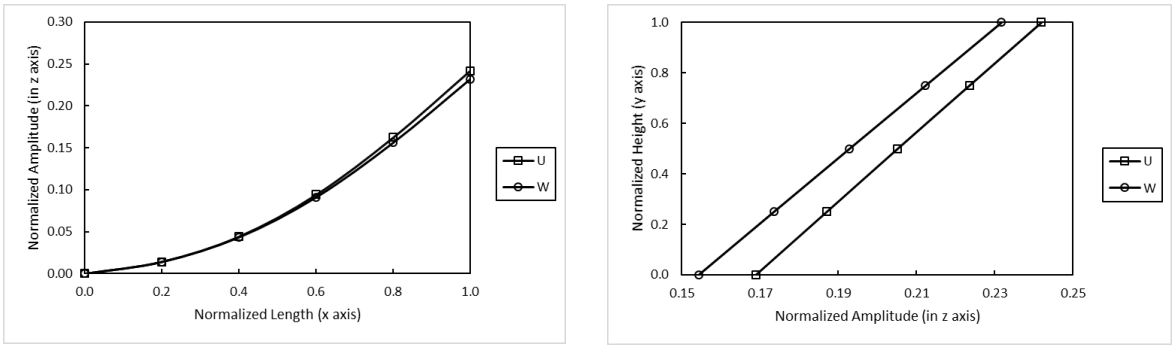

(a) in the *x*-*z* plane (b) in the *y*-*z* plane

Fig. 14 Mode shapes of plate in lateral buckling

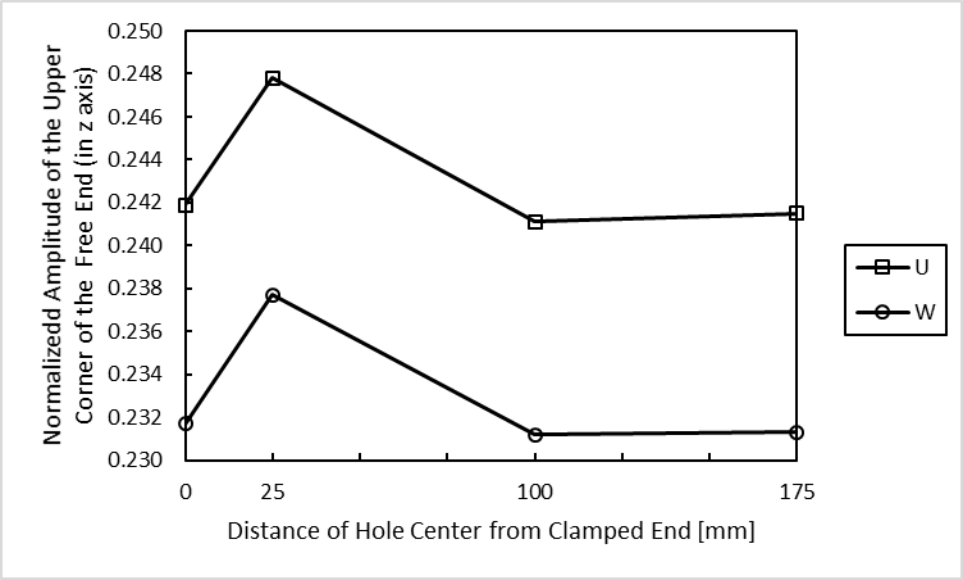

Fig. 15 Variations of normalized amplitude with hole location

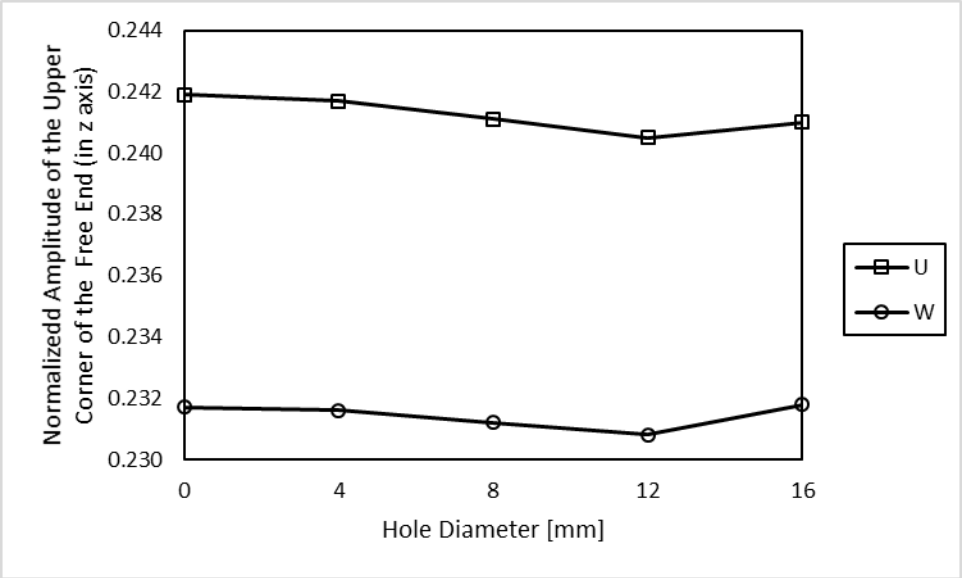

Fig. 16 Variations of normalized amplitude with hole diameter

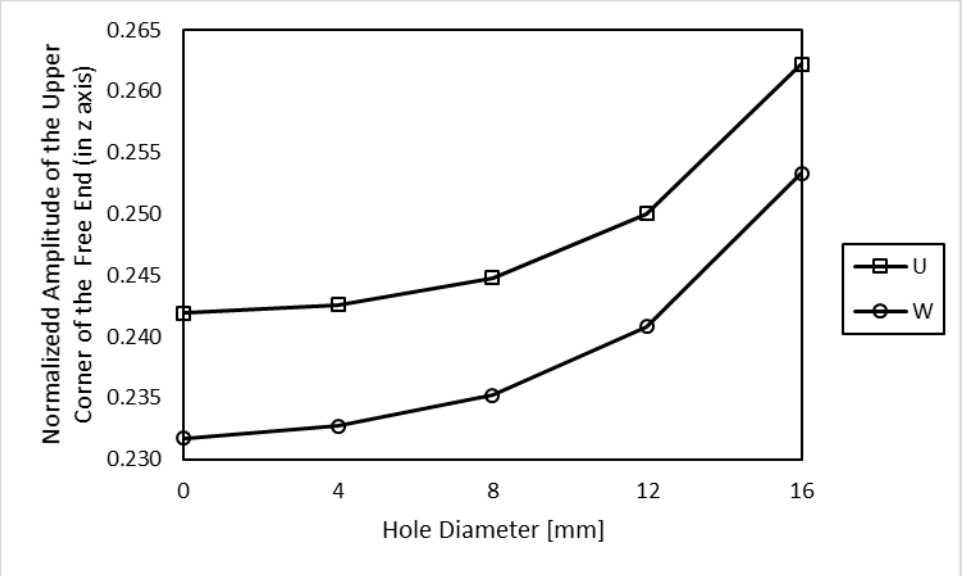

Fig. 17 Variations of normalized amplitude with hole number

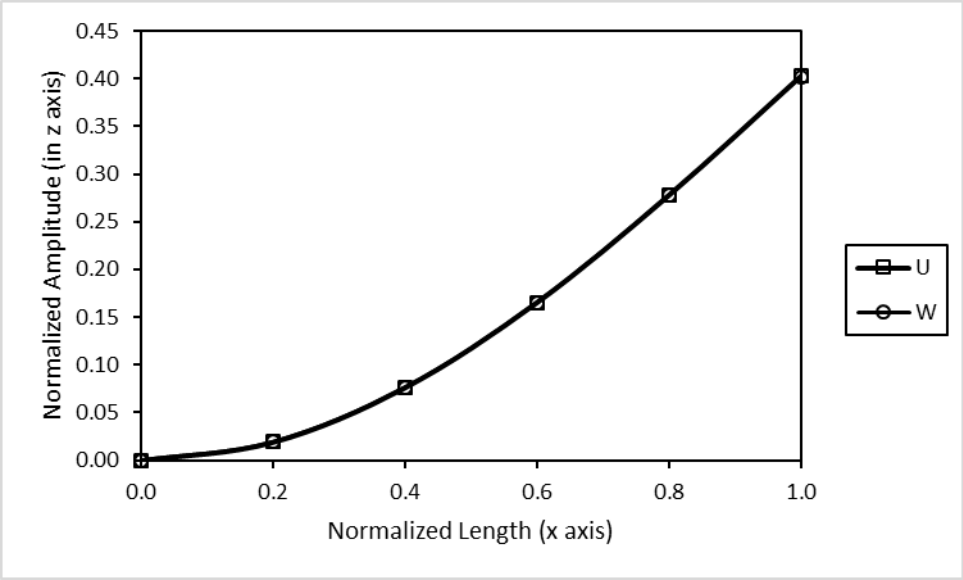

Fig. 18 Mode shapes of plate in longitudinal buckling

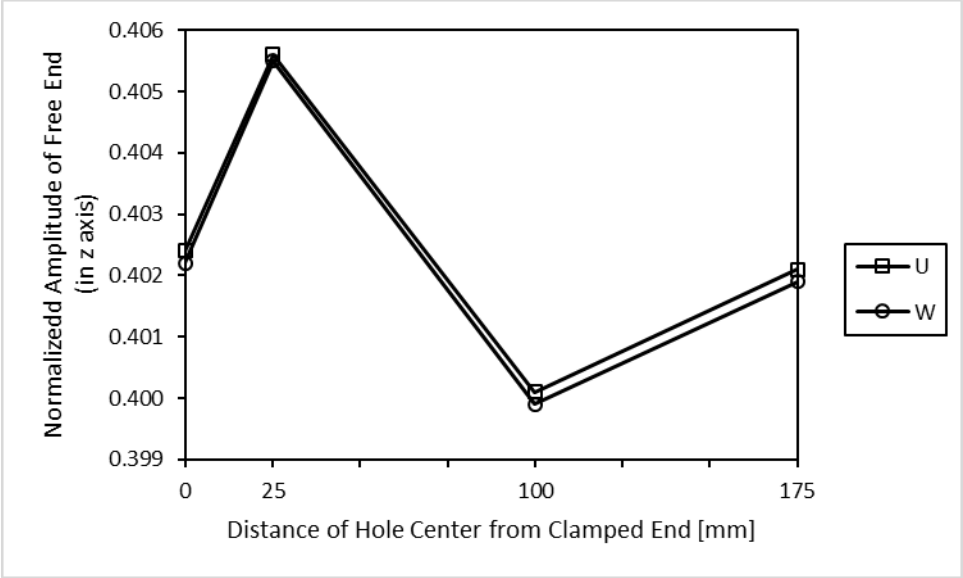

Fig. 19 Variations of normalized amplitude with hole location

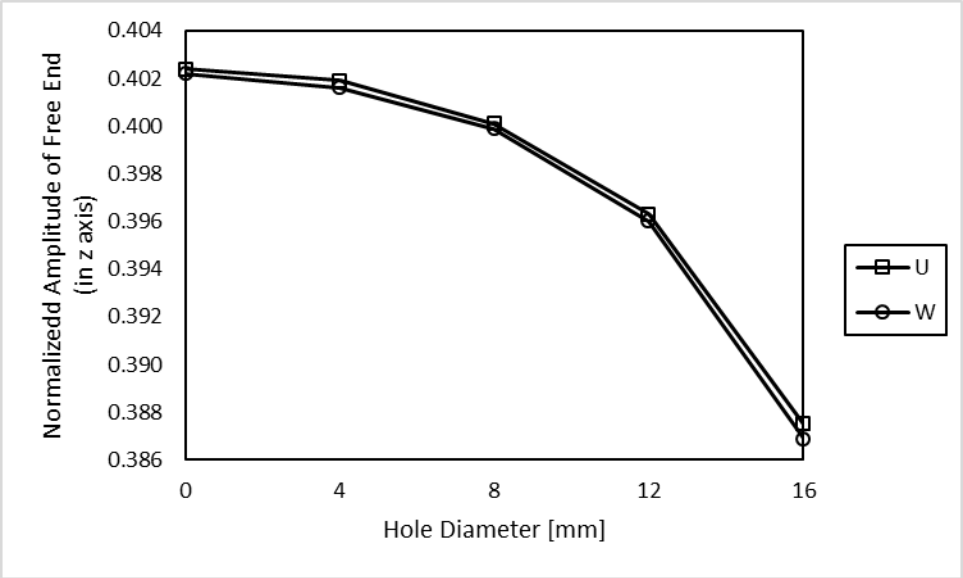

Fig. 20 Variation of normalized amplitude with hole diameter

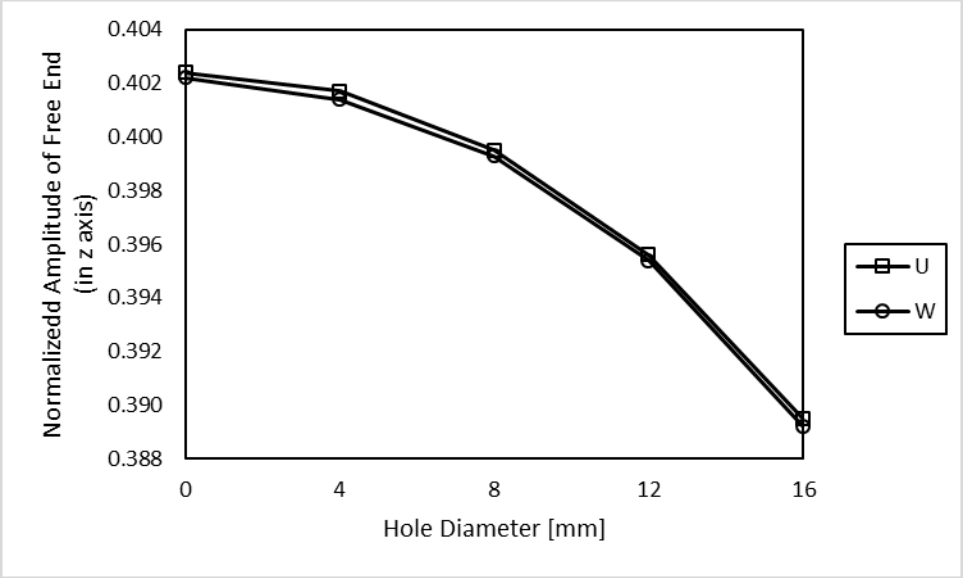

Fig. 21 Variation of normalized amplitude with hole number

TABLES

Table 1 The material properties of the composite fabrics [29].

Fabrics	E_1 [MPa]	E_2 [MPa]	G_{12} [MPa]	$G_{13}= G_{23}$ [MPa]	ρ [g/mm3]	ν_{12}	$\nu_{13} = \nu_{23}$
Unidirectional	20443	5184	1856	1113	0.001526	0.36	0.09
Woven	21651	21651	1646	988	0.001578	0.35	0.35

Table 2 Comparison of experimental and numerical results

Hole Status	Experiment Results [9]	Present Result (SolidWorks)	ANSYS Results	Percentage Difference (SolidWorks-ANSYS)	Percentage Error (Experimental-SolidWorks)
Unperforated	24.40	22.453	22.450	0.013	7.9795
	23.60				4.8602
	25.80				12.9729
Circular perforated	20.80	21.08	21.103	0.109	1.3462
	20.05				5.1372
	20.70				1.8357
Square perforated	19.06	20.384	20.413	0.142	6.9465
	18.93				7.6809
	19.85				2.6902